DOI: 10.1002/chem.200501176

Solubilization of Single-Walled Carbon Nanotubes by using Polycyclic Aromatic Ammonium Amphiphiles in Water—Strategy for the Design of High-Performance Solubilizers

Yasuhiko Tomonari,[a] Hiroto Murakami,[a] and Naotoshi Nakashima*[b]

Abstract: We describe the design of polycyclic aromatic compounds with high performance that dissolve single-walled carbon nanotubes (SWNTs). Synthetic amphiphiles trimethyl-(2-oxo-2-phenylethyl)-ammonium bromide (**1**) and trimethyl-(2-naphthalen-2-yl-2-oxo-ethyl)-ammonium bromide (**2**) carrying a phenyl or a naphtyl moiety were not able to dissolve/disperse SWNTs in water. By contrast, trimethyl-(2-oxo-2-phenanthren-9-yl-ethyl)-ammonium bromide (**3**) solubilized SWNTs, although the solubilization ability was lower than that of trimethyl-(2-oxo-2-pyrene-1-yl-ethyl)-ammonium bromide (**4**) (solubilization behavior observed by using **4** was described briefly in reference [4a]). Transmission electron microscopy (TEM), as well as visible/near-IR, fluorescence, and near-IR photoluminescence spectroscopies were employed to reveal the solubilization properties of **4** in water, and to compare these results with those obtained by using sodium dodecyl sulfate (SDS) and hexadecyltrimethylammonium bromide (HTAB) as solubilizers. Compound **4** solubilized both the as-produced SWNTs (raw-SWNTs) and purified SWNTs under mild experimental conditions, and the solubilization ability was better than that of SDS and HTAB. Near-IR photoluminescence measurements revealed that the chiral indices of the SWNTs dissolved in an aqueous solution of **4** were quite different from those obtained by using micelles of SDS and HTAB; for a SWNTs/**4** solution, the intensity of the (7,6), (9,5), and (12,1) indices were strong and the chirality distribution was narrower than those of the micellar solutions. This indicates that the aqueous solution of **4** has a tendency to dissolve semiconducting SWNTs with diameters in the range of 0.89–1.0 nm, which are larger than those SWNTs (0.76–0.97 nm) dissolved in the aqueous micelles of SDS and HTAB.

Keywords: adsorption · fluorescence spectroscopy · nanotubes · pi interactions · solubilization

Introduction

Since their first report in 1991,[1] carbon nanotubes (CNTs) have received much attention in nanoscience and nanotechnology because of their unique physical, chemical, mechanical, and electronic properties.[2] Due to the insolubility of CNTs in both aqueous and organic solvents, their applications are limited. Our interest has focused on noncovalent sidewall-functionalized soluble carbon nanotubes. Figure 1 shows the general idea for the solubilization of CNTs in solution,[3] in which the solubilizers are functional compounds that are composed of an aromatic moiety and a solvophilic moiety. In this concept, solubilizers carrying a hydrophilic or hydrophobic moiety are expected to dissolve CNTs in dipolar solvents, such as water and alcohols, and in nonpolar sol-

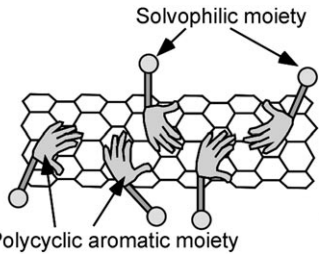

Figure 1. Strategy to solubilize SWNTs by physical adsorption of polycyclic aromatic molecules carrying a solvophilic moiety onto the surfaces of SWNTs.

[a] Y. Tomonari, Prof. Dr. H. Murakami
Department of Material Science
Graduate School of Science and Technology, Nagasaki University
Bunkyo, Nagasaki 852–8521 (Japan)

[b] Prof. Dr. N. Nakashima
Department of Chemistry and Biochemistry
School of Engineering, Kyushu University
744 Motooka, Fukuoka 819–0395 (Japan)
Fax: (+81) 92-802-2840
E-mail: nakashima-tcm@mbox.nc.kyushu-u.ac.jp

vents, respectively.[4] Reports describing solubilization by using aromatic compounds carrying pyrene,[4a,b,e,5] anthracene,[6] and porphyrin[4c,7] have been published.

In this paper, we describe the preparation of sidewall-functionalized water-soluble single-walled nanotubes (SWNTs) with four different polycyclic aromatic ammonium amphiphiles (**1**–**4**). Compounds **1** to **4** are water-soluble amphiphiles possessing a condensed cyclic number 1, 2, 3, and 4 for **1, 2, 3**, and **4**, respectively, and are suitable to demonstrate our general idea for the solubilization of CNTs in solution. We also used sodium dodecyl sulfate (SDS) and hexadecyltrimethylammonium bromide (HTAB) and compared their solubilization abilities toward SWNTs with those of **1**–**4**. Carbon nanotubes have been reported to be soluble in aqueous micellar solutions of such surfactants.[8]

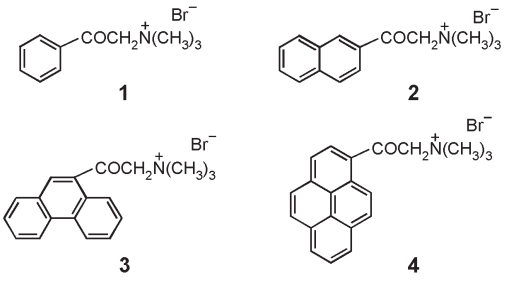

A preliminary report obtained by using compound **4** has been published elsewhere.[4a] We have also reported that the pyrene-carrying ammonium vinyl monomer and its copolymers,[4b] as well as some porphyrins,[4c] can solubilize SWNTs in water or organic solvents, and have described the importance of π–π interactions between the aromatic moieties and SWNT sidewalls toward the solubilization of SWNTs in solvents. Very recently, Guldi et al.[9] fabricated nanohybrids composed of SWNTs, compound **4**, and water-soluble metalloporphyrins, and reported that a rapid interhybrid charge separation causes the reduction of the electron-accepting SWNTs and the oxidation of the electron-donating porphyrin. They also described the photoelectrochemical behaviors at an indium tin oxide (ITO) electrode modified with a nanocomposite of SWNTs–compound **4**–polythiophene carboxylate.[10] We[4c] reported that zinc protoporphyrin IX solubilizes SWNTs in DMF. Sun et al.[11] described that 5,10,15,20-tetrakis(hexadecyloxyphenyl)-21*H*,23*H*-porphine selectively interacts with semiconducting SWNTs in chloroform. Paloniemi et al.[12] examined the solubilization behaviors of SWNTs by using several kinds of aromatic compounds and found that naphthalene groups carrying amino and sulfonyl groups can dissolve SWNTs in water.

Experimental Section

Materials: SDS, HTAB, and as-produced SWNTs (raw-SWNTs) were purchased from Nacalai Tesque, Wako Chemical Industries, and Carbon Nanotechnologies, respectively, and were used as received. The length and diameter of raw-SWNTs were approximately 1–10 μm and 0.7–1.2 nm, respectively.

Syntheses

*Trimethyl-(2-oxo-2-phenylethyl)-ammonium bromide (**1**)*: An excess amount of trimethylamine gas was introduced into 2-bromoacetophenone (0.112 g, 0.56 mmol) in dry THF (15 mL) at RT, and the solution was stirred for 1 d. The precipitate was separated and dried in a vacuum to give **1** as a white solid, 84%. ^{1}H NMR (300 MHz, [D$_4$]CD$_3$OD): δ = 7.5–8.4 (m, 5H; PhH), 3.4 ppm (s, 9H; (CH$_3$)$_3$N$^+$); IR (KBr): $\tilde{\nu}$ = 3054, 3000, 1689 cm^{-1}; elemental analysis calcd (%) for C$_{11}$H$_{16}$NOBr: C 51.61, H 6.25, N 5.43; found: C 50.91, H 6.25, N 5.39.

*Trimethyl-(2-naphthalene-2-yl-2-oxo-ethyl)-ammonium bromide (**2**)*: An excess amount of trimethylamine gas was introduced into 2-bromo-2′-acetonaphtone (0.134 g, 0.53 mmol) in dry THF (15 mL) at RT, and the solution was stirred for 1 d. The precipitate was separated and dried in a vacuum to give **2** as a white solid, 73%. ^{1}H NMR (300 MHz, [D$_4$]CD$_3$OD): δ = 7.6–8.6 (m, 7H; PhH), 3.4 ppm (s, 9H; (CH$_3$)$_3$N$^+$); IR (KBr): $\tilde{\nu}$ = 3054, 3008, 1697 cm^{-1}; elemental analysis calcd (%) for C$_{15}$H$_{18}$NOBr: C 58.44, H 5.89, N 4.54; found: C 58.90, H 6.06, N 4.50.

*Trimethyl-(2-oxo-2-phenanthrene-9-yl-ethyl)-ammonium bromide (**3**)*: An excess amount of trimethylamine gas was introduced into 9-(2-bromoacetyl)phenanthrene (0.100 g, 0.33 mmol) in dry THF (15 mL) at RT, and the solution was stirred for 1 d. The precipitate was separated and dried in a vacuum to give **3** as a white solid, 88%. ^{1}H NMR (300 MHz, [D$_4$]CD$_3$OD): δ = 7.7–8.9 (m, 9H; PhH), 3.5 ppm (s, 9H; (CH$_3$)$_3$N$^+$); IR (KBr): $\tilde{\nu}$ = 3000, 1697 cm^{-1}; elemental analysis calcd (%) for C$_{19}$H$_{20}$NOBr: C 63.68, H 5.63, N 3.91; found: C 63.50, H 5.69, N 3.84.

*Trimethyl-(2-oxo-2-pyrene-1-yl-ethyl)-ammonium bromide (**4**)*: The synthetic method of **4** was briefly described in a previous paper.[4a] An excess amount of trimethylamine gas was introduced into 1-(bromoacetyl)pyrene (0.191 g, 0.59 mmol) in dry THF (15 mL) at RT, and the solution was stirred for 1 d. The precipitate was separated and dried in vacuum to give **4** as a yellow solid, 87%. ^{1}H NMR (300 MHz, [D$_4$]CD$_3$OD): δ = 8.1–9.1 (m, 9H; PyH), 4.1 (s, 2H; CH$_2$N$^+$), 3.6 ppm (s, 9H; (CH$_3$)$_3$N$^+$); IR (KBr): $\tilde{\nu}$ = 3045, 3012, 1674 cm^{-1}; elemental analysis calcd (%) for C$_{21}$H$_{20}$NOBr·1.2H$_2$O: C 62.45, H 5.59, N 3.47; found: C 62.16, H 5.21, N 3.06.

Purification of raw-SWNTs:[13] Raw-SWNTs (HiPco) were heated at 225 °C in humid air, and then the samples were sonicated by using an ultrasonic cleaner (Branson 5510) in concd aqueous HCl. The nanotubes were then collected by using a porous filter (Advantec PTFE; pore size, 100 nm), and then washed with sodium hydrogen carbonate. SWNTs were collected by using a porous filter (Advantec, PTFE; pore size, 100 nm), and then dried at 50 °C to obtain the purified SWNTs (p-SWNTs), which were used for further experiments. Analysis of these nanotubes by X-ray photoelectron spectroscopy (XPS) revealed no peak for Fe$_{2p3/2}$ in the region of 706–714 eV, indicating that the Fe was almost removed by this purification procedure.

Solubilization/dispersion of SWNTs: Typical solubilization procedures are as follows: Raw-SWNTs or p-SWNTs (≈1.0 mg) were placed in an aqueous solution of **1** (or **2, 3, 4**, each 1 mM), HTAB (29 mM), or SDS (10 and 36 mM), followed by sonication in a bath-type sonicator (Branson 5510) for 1 h, and then optional sonication in a cup-horn sonicator (SMT, UH-300) for 10 min at RT. After sonication, the samples were centrifuged (SIGMA, 3K30C or HITACHI KOKI, CS100GXL) at a given g-value. The upper 70–80% of supernatant was then carefully decanted.

Resolubilization of SWNTs/4 nanocomposite: An aqueous dispersion/solution of SWNTs/**4** was passed through a filter (Advantec, PTFE; pore size, 100 nm), and a residue (solid) on the filter paper was rinsed well with D$_2$O. The collected solid was placed in D$_2$O, and then sonicated in a bath-type sonicator (Branson 5510) for 10 min to produce a black, transparent aqueous solution/dispersion.

Transmission electron microscopy (TEM) and atomic force microscopy (AFM): Typical procedures are as follows: A carbon-coated TEM grid (Ouken-Shoji, 200-A mesh) was immersed in an aqueous solution of SWNTs/**4** for a few seconds and then air-dried. TEM measurements were conducted by using a Jeol JEM-100S electron microscope. An aqueous

solution of SWNTs/**4** was dropped onto a cleaved mica substrate, rinsed with pure water (Milli-Q Plus Ultrapure water system, Millipore), and then dried in vacuum before measurement. AFM images were recorded by using a SPI 3800N (Seiko Instruments) with a Si_3N_4 cantilever (SN-AF01).

Raman spectroscopy: Raman spectra for SWNTs were recorded by using a Renishaw Ramanscope System 1000 (excitation wavelength, 514.5 nm of an Ar ion laser).

Vis/near-IR (NIR) absorption and fluorescence spectroscopy of individually dissolved SWNTs: Raw-SWNTs and an aqueous solution of **4** (or SDS or HTAB) were sonicated in a bath-type sonicator (Branson 5510) for 1 h, and then in a cup-horn sonicator (SMT, UH-300) for 10 min at RT. After centrifugation (HITACHI KOKI, CS100GXL) for 4 h at 118000 g, the supernatant was carefully separated. NIR fluorescence spectra were recorded by using a HORIBA SPEX Fluorolog-3-NIR spectrofluorometer equipped with a liquid-nitrogen-cooled InGaAs near-IR detector. Excitation and emission wavelengths were 500–900 and 900–1300 nm, respectively.

Thermogravimetric analysis (TGA): TGA curves (10 °C min^{-1}) were recorded by using a Shimazu TGA-50H instrument.

Results and Discussion

Solubilization/dispersion of raw-SWNTs: The solubilization/dispersion of raw-SWNTs in water containing **1, 2, 3**, or **4** was carried out by using the typical procedure described in the Experimental Section to obtain SWNTs/**1**, SWNTs/**2**, SWNTs/**3**, and SWNTs/**4**. A photograph of the four solutions obtained is shown in Figure 2. Although the photo of the SWNTs dissolved in an aqueous solution of **4** has already been reported,[4a] it is displayed again in Figure 2d for the purpose of comparison with the solutions obtained by using **1**–**3**. Compound **3**, a tricyclic aromatic amphiphile, gave a pale-black solution (Figure 2c). In contrast, as can be seen in Figure 2a and b, the use of **1** and **2** gave colorless solutions. We measured Raman spectra for SWNTs obtained from solutions of SWNTs/**3** and SWNTs/**4** and for insoluble SWNTs separated from solutions of **1** and **2** containing SWNTs. As shown in Figure 3, the four spectra obtained (b–e) resemble that of the original SWNTs (a) and the intensity ratios of the G-band/D-band of the five spectra differ only slightly, indicating that functionalization did not damage the tubes themselves.

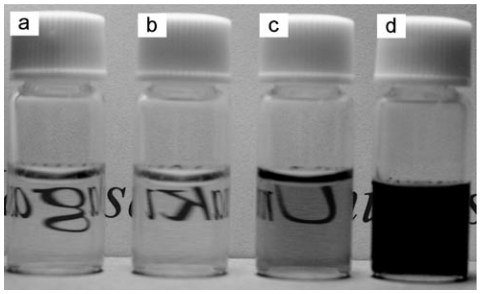

Figure 2. Aqueous solutions of raw-SWNTs/**1** (a), raw-SWNTs/**2** (b), raw-SWNTs/**3** (c), and raw-SWNTs/**4** (d).

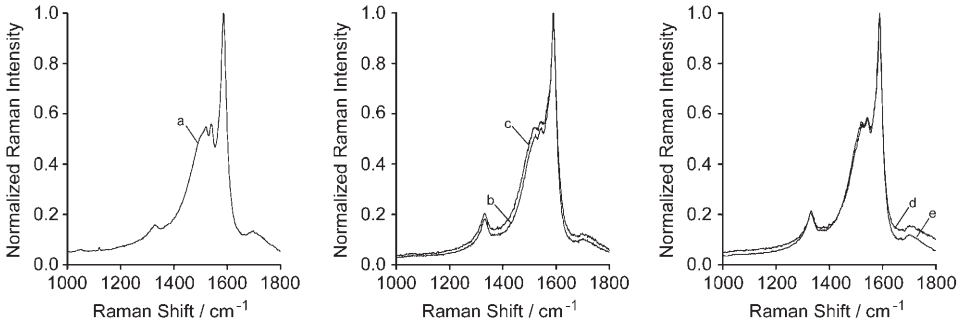

Figure 3. Raman spectra for raw-SWNTs (a), insoluble raw-SWNTs (b and c) separated from solutions of SWNTs/**1** and SWNTs/**2**, respectively, and the solid products (d and e) obtained from solutions of raw-SWNTs/**3** and raw-SWNTs/**4**, respectively.

Figure 4 shows typical visible/near-IR spectra of the four different solutions/dispersions containing SWNTs/**1**, SWNTs/**2**, SWNTs/**3**, and SWNTs/**4**, in which deuterated water was used in place of normal water, as water absorbs in the near-IR region. Aqueous solutions of SWNTs/**3** and SWNTs/**4** showed characteristic absorption bands in the visible/near-IR regions, due to the interband transition between the mirror image spikes in the density of states (DOSs)[14] of the SWNTs. In contrast, almost no absorbance was detected upon use of compounds **1** and **2**, indicating that these compounds did not act as SWNT solubilizers. The number of

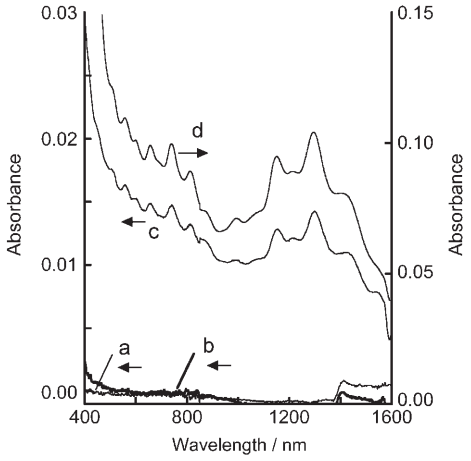

Figure 4. Vis/near-IR absorption spectra of D_2O solutions/dispersions of raw-SWNTs/**1** (a), raw-SWNTs/**2** (b), raw-SWNTs/**3** (c), and raw-SWNTs/**4** (d). Optical cell length: 1 mm, concentration of **1, 2**, and **3**: 1.0 mM.

condensed polycyclic aromatic rings in **1**–**4** is crucial for the solubilization of the SWNTs in water. It is evident that both the phenyl and naphthalene groups are noneffective chromophores in the design of SWNT solubilizers. Recently, Paloniemi et al.[12] reported that naphthalene derivatives with an amino group could disperse SWNTs in solvent, and they indicated the contribution of a charge-transfer interaction between the amino group and the SWNTs.

We have examined the effect of solvent on the solubilization of SWNTs. Unfortunately, the solubility of compound **4** is limited, namely it is soluble in water, water/methanol, and water/DMF, but insoluble in methanol, DMF, and other many solvents. Therefore, we carried out experiments by using D_2O/CD_3OD (9:1, v/v) and D_2O/DMF (9:1, v/v) in place of D_2O, and found that SWNTs can be solubilized in these solvents (data not shown).

As we described elsewhere,[4a] the absorption maxima of the UV-visible spectra of the SWNTs/**4** solution appeared at 234, 288, and 368 nm together with a shoulder at 400 nm, which are almost identical to those of the **4** aqueous solution only. This result suggests that the spectrum was governed by **4** in the bulk solution. The UV-visible spectrum of SWNTs/**3** was also virtually identical to that of the aqueous solution of **3** containing no SWNTs. The spectral shift of **4** bound to the surfaces of the SWNTs is discussed below. Compound **4** is not a micelle-forming amphiphile in water, and neither is compound **3** because, from surface-tension measurements, no critical micelle concentration (cmc) was observed in an aqueous solution of **3**. Therefore, the solubilization of the SWNTs obtained by using compounds **3** and **4** is not by means of the so-called "micelle dissolution", but instead, physical adsorption through π–π interaction of the polycyclic aromatic moiety and the sidewalls of the SWNTs is suggested to play an important role in solubilization. The details of the mechanism of the solubilization of the SWNTs are discussed below.

Transmission electron microscopy (TEM) and atomic force microscopy (AFM) were performed to reveal the structures of the raw-SWNTs dissolved in water containing **3** or **4**. We used a cationic surfactant, HTAB, and compared the results to those obtained by using **3** and **4**. Typical examples of the TEM images obtained are shown in Figure 5, in which many catalyst particles of iron are seen upon using HTAB as a solubilizer. By comparison, such particles were scarce in the solutions of both SWNTs/**3** and SWNTs/**4**, indicating that compounds **3** and **4** were effective for not only the dissolution, but also in purification of the raw-SWNTs. Figure 5d and e show images of insoluble raw-SWNTs separated from solutions of **1** and **2**, respectively, in which SWNTs are seen to contain a lot of metal nanoparticles. These images resemble that of the used raw-SWNTs in the absence of the functionalization procedure. We conducted thermogravimetric analysis (TGA) experiments for the raw-SWNTs and for the SWNTs obtained from a solution containing **4** and SWNTs after centrifugation at 60000 g for 2 h. The Fe contents in these two samples were 28 and 10%, respectively.

A typical AFM image on mica obtained from a SWNTs/**4** solution is shown in Figure 6. From the height profile of the image, we observe a large percentage of the SWNTs whose diameters are approximately 1–1.5 nm, indicating that the SWNTs are individually dissolved in water.

Comparison of raw-SWNTs and purified (p)-SWNTs: Hauge et al.[13] reported that raw-SWNTs have a tendency to form strong bundled structures during purification processes. Hence, it is suggested that the solubilization behaviors of the raw-SWNTs and p-SWNTs are different. We examined the solubilization ability of **4** toward the raw- and p-SWNTs and compared the results with those obtained by using SDS. As shown in Figure 7, following sonication in a bath-type sonicator, the solubilization behaviors of the raw-

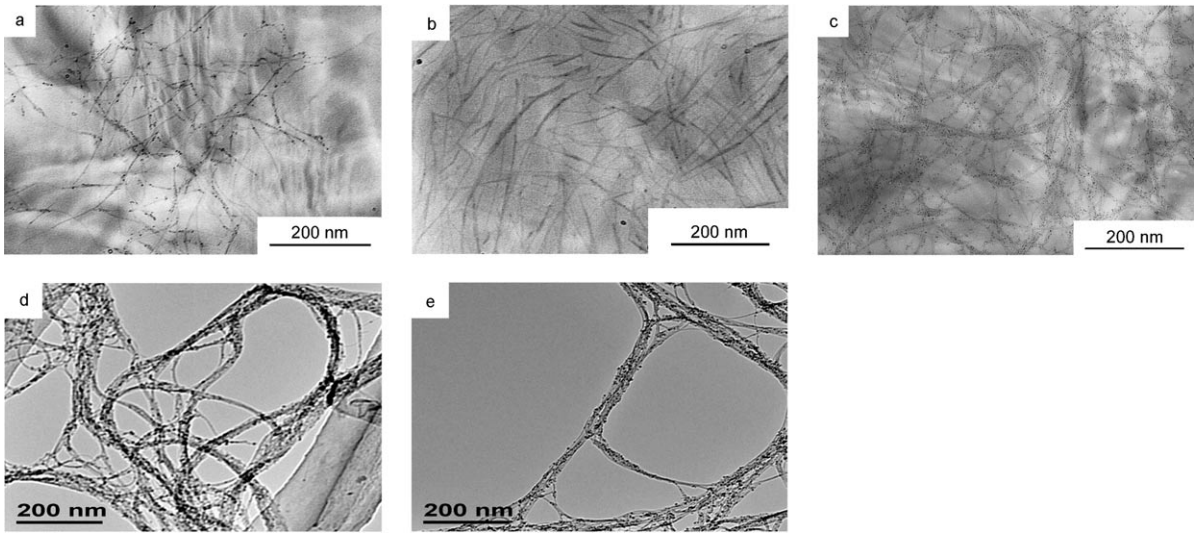

Figure 5. TEM images of aqueous solution/dispersions of raw-SWNTs/**3** (a), raw-SWNTs/**4** (b), raw-SWNTs/HTAB (c), and insoluble raw-SWNTs (d and e) separated from solutions of **1** and **2**, respectively.

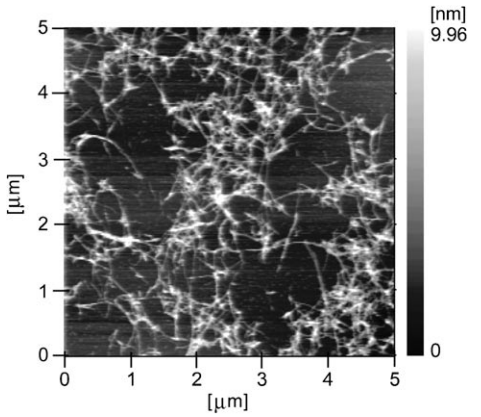

Figure 6. Typical AFM image of an aqueous solution of raw-SWNTs/**4**.

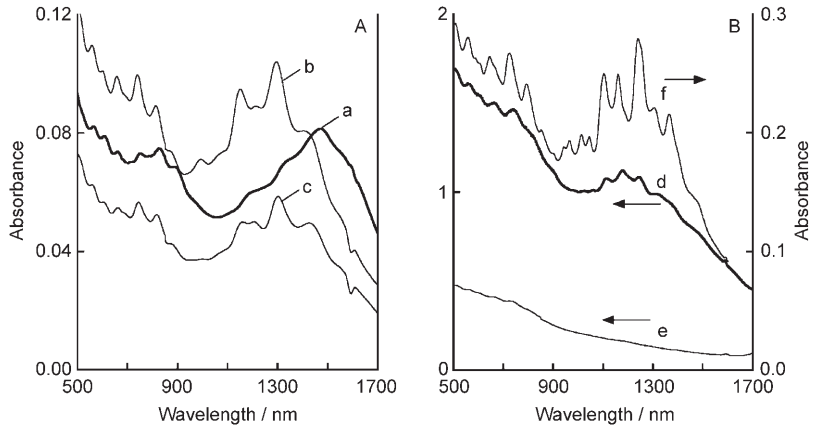

Figure 7. Vis/near-IR absorption spectra for D_2O solutions of SWNTs/**4** (A) and SWNTs/SDS (B). The p-SWNTs and the raw-SWNTs were used for spectral measurements a, b, d, e, and c, f, respectively. Sample-preparation conditions for (a)–(f): sonication in a bath-type sonicator for 1 h, followed by centrifugation at 1000 g for 30 min (a and d); sonication in a bath-type sonicator for 1 h and then in a cup-horn sonicator for 10 min, followed by centrifugation at 1000 g for 30 min (b and e); sonication in a bath-type sonicator for 1 h and then in a cup-horn sonicator for 10 min, followed by centrifugation at 60000 g for 4 h (c and f). Optical cell length, 1.0 mm.

SWNTs (spectrum c) and p-SWNTs (spectrum a) were quite different. The S1 band of the p-SWNTs appeared in the region of 1200–1700 nm, which was shifted largely to the longer wavelength compared to that of the raw-SWNTs, and the band was not well-resolved. These results suggested that the p-SWNTs formed bundled structures under these experimental conditions. The effect of the sonication power on the combination of p-SWNTs and the solubilizer **4** was examined. This revealed that additional sonication for 10 min in a cup-horn type sonicator following sonication in the bath-type sonicator caused a drastic change in the spectral shape and, as shown in spectrum b in Figure 7, the spectrum obtained was almost identical to that of the raw-SWNTs. We wish to emphasis that both the raw- and p-SWNTs can be readily solubilized under the "mild" experimental conditions. The use of SDS micelles for the dissolution of the raw-SWNTs and sonication in both a bath-type sonicator and a cup-horn sonicator, followed by centrifugation at 60000 g produced dissolution giving the well-resolved near-IR spectrum (spectrum f in Figure 7) that was virtually identical to reported data.[8c] However, for the p-SWNTs, the spectrum obtained was broad (spectra d and e in Figure 7). Evidently, compound **4** is a better solubilizer than SDS for p-SWNTs.

The effect of centrifugation on the dissolution of the raw-SWNTs by using **4** was examined. We varied the g-values from 1000 to 120000 g. Approximate SWNT solubility values obtained in aqueous solutions of **4** prepared by centrifugation at 1000 and 60000 g were 0.028 and 0.010 mg mL^{-1}, respectively. As exhibited in Figure 8, the absorbance for the four SWNT aqueous solutions decreased as the g-values increased, and all gave resolved spectra whose shapes and peak maxima varied little. The fact that centrifugation at much lower g-values (~1000 g) was effective for the preparation of individually dissolved SWNTs in water is important for obtaining large amounts of individually dissolved SWNTs.

Fluorescence from pyrene: Pyrene-carrying compounds are often used as fluorescence probes because the fluorescence quantum yield of pyrene is high.[15] We measured the fluorescence spectra of aqueous solutions of **4** in the absence or presence of the raw-SWNTs. At lower concentrations of **4** below 10^{-6} M, only monomer emission spectra were observed at around 421 nm, and at concentrations above 10^{-5} M, excimer emis-

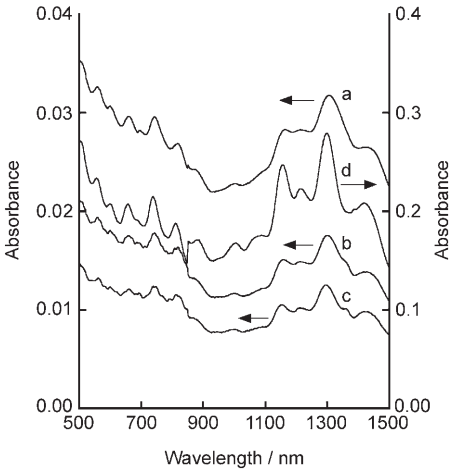

Figure 8. Vis/near-IR absorption spectra of aqueous solutions of raw-SWNTs/**4** prepared by sonication in a bath-type sonicator for 1 h, followed by centrifugation at 1000 g for 2 h (a), 10000 g for 2 h (b), 60000 g for 2 h (c), and 118000 g for 2 h (d). Optical cell length, 1.0 mm for (a)–(c) and 10 mm for (d).

sions were observed at around 501 nm together with monomer emissions at around 421 nm. Unfortunately, the observed fluorescence behaviors of the raw-SWNTs/**4** solution were virtually the same as those of the **4** aqueous solution alone, suggesting that the fluorescence from the SWNTs/**4** solution is derived from the nonbound (free) **4** in the solution. To remove the free **4** molecules (not bound to the SWNTs), the solution was filtered by using filter paper. The resulting solid was then resolubilized in pure water by sonication in a bath-type sonicator (for details, see Experimental Section). The UV/visible/near-IR spectrum for the resolubilized solution obtained is shown in Figure 9, together with

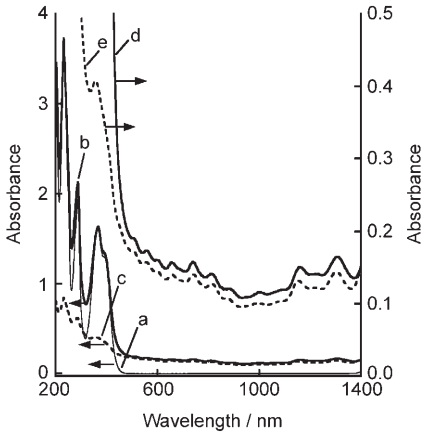

Figure 9. UV/Vis/near-IR absorption spectra for aqueous solutions of **4** (a), raw-SWNTs/**4** (b and d), and resolubilized raw-SWNTs/**4** (c and e). The spectra of (d) and (e) are magnifications of (b) and (c), respectively. Optical cell length, 1.0 mm.

the spectra for a SWNTs/**4** solution before resolubilization and for an aqueous solution of **4** only. From the data, the concentration of **4** in the resolubilized solution was calculated to be approximately 0.24 mM, which means a decrease of 75% from the original concentration. The resolubilized solution obtained was stable for more than three months in a refrigerator, that is, no precipitate was produced during this period. On the other hand, the decrease in absorbance of the SWNTs in the resolubilized solution in the near-IR region was only 11%. The peak maxima of pyrene moieties in the resolubilized solution appeared at 232, 287, and 357 nm, which are somewhat different from the original solution (peak maxima: 232, 288, and 367 nm). For the resolubilized solution, the observed blue-shift of approximately 10 nm in the region of 360 nm together with the decrease in the shoulder peak near 400 nm relative to the original solution is due to a π–π interaction between the SWNT sidewalls and the pyrene moiety.

Fluorescence spectra provided direct evidence for the interaction between compound **4** and the SWNTs. As shown in Figure 10, the excimer emission from the pyrene moiety in the resolubilized solution was drastically quenched compared to that of the original solution, suggesting an energy transfer from the pyrene moiety on **4** to the SWNTs. We

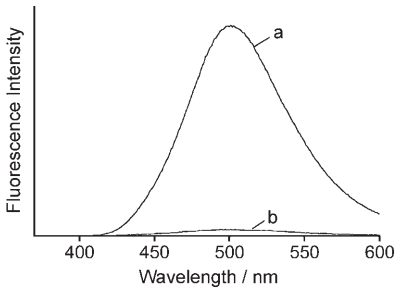

Figure 10. Fluorescence spectra of an aqueous solution of **4** ([**4**] = 0.24 mM) (a) and a resolubilized aqueous solution of SWNTs/**4** (b) (concentration of **4** was estimated to be 0.24 mM). Excitation wavelengths for (a) and (b) are 367 and 357 nm, respectively.

compared the fluorescence intensity of solutions in the absence and presence of SWNTs possessing the same absorbance of the pyrene chromophore. We have already reported a similar fluorescence quenching of zinc protoporphyrin IX adsorbed on the surface of the SWNTs in a DMF solution.[4c] Sun et al.[17] synthesized SWNTs tethered with pyrenes and observed the quenching of pyrene emission in solution. This quenching was explained by energy transfers from the tethered pyrene moieties to the nanotubes. They also synthesized SWNTs tethered with porphyrins and described the quenching of porphyrin emission as well as energy transfers from the tethered porphyrins to the nanotubes. On the other hand, Murray et al.[6a] reported that anthracene adsorbed on SWNTs in THF is strongly luminescent. Hedderman et al.[6b] also described that the fluorescence from anthracene adsorbed on the SWNTs was not much different from that observed in the absence of SWNTs. The fluorescence behaviors from fluorophores adsorbed on the surface of nanotubes remain complex.

Photoluminescence from SWNTs: Smalley et al.[8c] and Weisman et al.[8d] reported that raw-SWNTs dissolved in an aqueous micelle of SDS showed individual photoluminescence in the near-IR region. Since these reports were published, considerable attention has been focused on these unique optical behaviors. We measured the near-IR photoluminescence spectra of SWNTs dissolved in an aqueous (deuterated) solution of **4**, and compared the results to those obtained by using aqueous micelles of SDS and HTAB. Three sample solutions were prepared under the same experimental conditions, namely, by sonication in a bath-type sonicator for 1 h followed by sonication in a cup-horn sonicator for 10 min and then ultracentrifugation at 118000 g for 4 h. The three samples obtained exhibited photoluminescence in the near-IR region and the contour plots of the excitation wavelength (500–900 nm)/emission wavelength (900–1300 nm) profile are demonstrated in Figure 11. The contour plot for SWNTs/SDS proved the existence of SWNTs with chiral indices of (7,6), (8,6), (9,4), and (9,5), which resembled those previously reported.[18] However, there were some differences: in the literature, the (9,5) index was not detected and the intensity of (7,5) in our SDS sample was weaker than

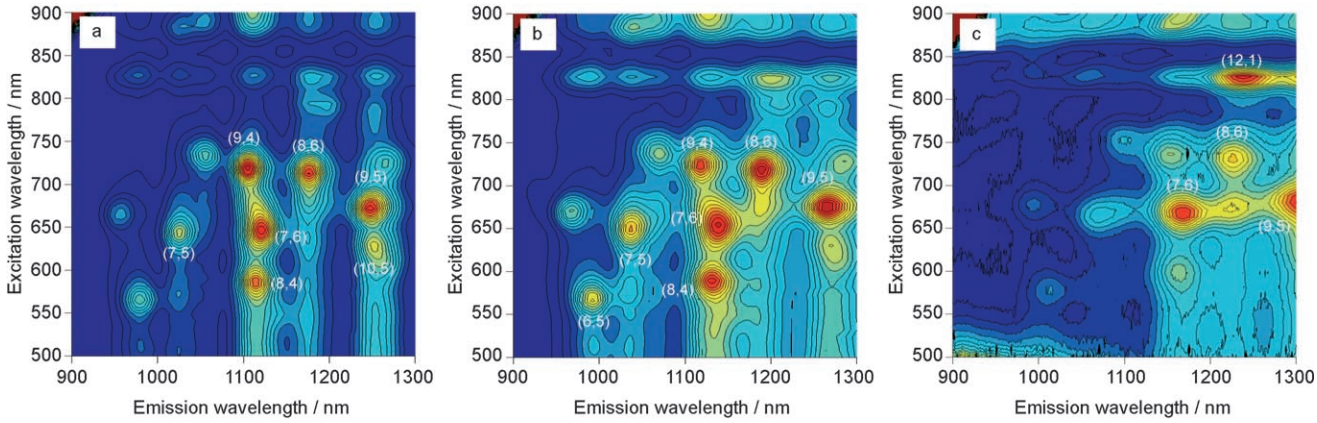

Figure 11. Contour plots of photoluminescence spectra for D_2O solutions of raw-SWNTs/SDS (a), raw-SWNTs/HTAB (b), and raw-SWNTs/**4** (c) as a function of excitation and emission wavelengths.

that reported in the literature. This difference could be due to the experimental procedure and lot numbers of HiPco SWNTs obtained from Carbon Nanotechnologies. As shown in Figure 11a and b, SWNTs/SDS and SWNTs/HTAB gave very similar contour plots, whereas SWNTs/**4** produces a differently patterned contour plot (Figure 11c), in which the intensity of the (7,6), (9,5), and (12,1) indices were strong and the intensity of (8,6) was weaker than those from SWNTs/SDS and SWNTs/HTAB. Notably, the index (12,1) in Figure 11c is not detected in plots a and b. The diameter of SWNTs with the index (12,1) corresponds to 0.995 nm, which is the largest diameter among the observed indices. The π–π interaction between the (12,1) SWNTs and compound **4** might play a role in the solubilization of the nanotubes. One more characteristic feature observed for SWNTs/**4** is a red-shift in the spectra relative to those of SWNTs/SDS and SWNTs/HTAB. Smalley et al.[8f] measured the near-IR photoluminescence of individually dissolved SWNTs in micelles of various surfactants. They found that SDS and sodium dodecylbenzene sulfate gave the bluest-shifted spectra, and HTAB and Brij 700 showed a red-shift. They described that water at the nanotubes surface causes a shift in the fluorescence peak.

Mechanism of solubilization: As we described above for the solubilization/dispersion of the raw-SWNTs, the mechanism for solubilization with **4** is different from the so-called "micellar solubilization" with surfactants. In the latter, the adsorption of a hemimicelle onto the nanotube is believed to be important for the solubilization of the nanotubes, and the surfactant molecules are in dynamic equilibrium between the bulk phase and the sidewalls of the SWNTs. We conducted a dialysis experiment for a SWNTs/**4** aqueous solution by using membrane tubing (molecular weight cut-off 3500, Spectrapor Spectrum Medical Industries). The solubilizer **4** leaked gradually from the inside of the tubing to the outer water phase and caused precipitation of the SWNTs within the tubing. These results indicate that molecules of **4** are in a state of dynamic equilibrium between the surfaces of the SWNTs and the bulk solution. Fluorescence spectroscopy revealed that the excimer emission from the pyrene moiety on **1** in the resolubilized solution was quenched drastically relative to that of the original solution. Taken together, one possible model for the solubilization with **4** is presented in Figure 12, in which the adsorption of the monomer and dimer of the solubilizer onto the surfaces of SWNTs is drawn schematically. Here, the adsorption of the pyrene moiety onto the SWNTs through a π–π interaction plays an important role in solubilization. A minor contribution of the cation–π interaction[12,19] between the ammonium moiety and the SWNTs might need to be considered. The simple mechanism presented would be applicable to a variety of aromatic amphiphiles, such as compound **3**.

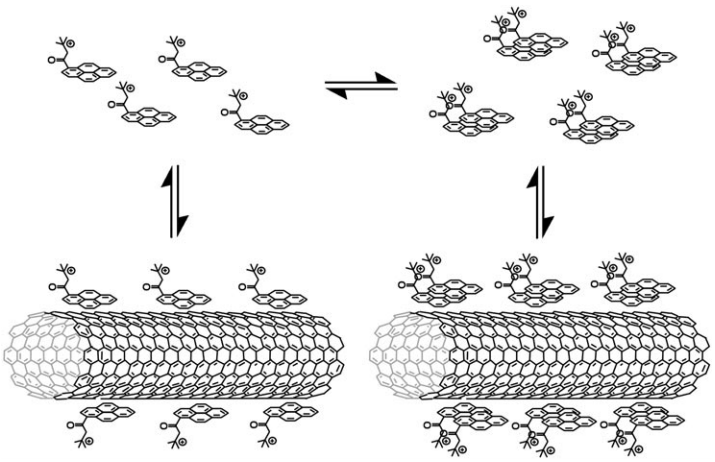

Figure 12. Possible mechanism for the solubilization of SWNTs with **4**.

Conclusion

We have described the importance of the condensed polycyclic aromatic moiety in the design of carbon-nanotube solubilizers. Ammonium amphiphiles carrying a phenyl or naphthyl group did not act as carbon-nanotube solubilizers; in-

stead, the phenanthlyl and pyrenyl groups play an important role in the solubilization. Pyrene ammonium (**4**), an amphiphile that does not form micelles, acted as an excellent solubilizer for both the raw-SWNTs and p-SWNTs. Aqueous solutions of SWNTs/**4** exhibited interesting fluorescence properties. The efficient fluorescence quenching of the pyrene chromophore suggested energy transfer from the pyrene group chemisorbed on the SWNTs to the SWNTs. The most interesting feature is the selective dissolution of SWNTs by **4**, indicated by the near-IR photoluminescence measurements that revealed that the aqueous SWNTs/**4** possesses (7,6), (9,5), and (12,1) indices. This means that aqueous solution of **4** has a tendency to dissolve semiconducting SWNTs with diameters in the range of 0.89–1.0 nm. These were larger than those of aqueous micelles of SDS and HTAB (diameter range of 0.76–0.97 nm). This fine discrimination in the diameters of the SWNTs is of interest in the design of nanotube solubilizers that recognize a single nanotube chiral index, as the synthesis of SWNTs with a single chiral index is presently difficult, and also for their potential applications in many fields of science and technology.

Acknowledgements

We thank Prof. H. Furuta of Kyushu University for the use of a HORIBA SPEX Fluorolog-3-NIR spectrofluorometer and Prof. S. Maruyama and Mr. Y. Miyauchi of The University of Tokyo for their technical assistance in the preparation of the contour plots of the photoluminescence data. This work was supported by Grants-in-Aid from the Japanese Ministry of Education, Science, Sports, and Culture.

[1] S. Iijima, *Nature* **1991**, *354*, 56.
[2] a) *Carbon Nanotubes and Related Structures* (Ed.: P. J. F. Harris), Cambridge University Press, Cambridge, **1999**; b) *The Science and Technology of Carbon Nanotubes* (Eds.: K. Tanaka, T. Yamabe, K. Fukui), Elsevier, Oxford, **1999**; c) S. Niyogi, M. A. Hamon, H. Hu, B. Zhao, P. Bhowmik, R. Sen, M. E. Itkis, R. C. Haddon, *Acc. Chem. Res.* **2002**, *35*, 1105; d) A. Hirsch, *Angew. Chem.* **2002**, *114*, 1933; *Angew. Chem. Int. Ed.* **2002**, *41*, 1853; e) S. Banerjee, M. G. C. Kahn, S. S. Wong, *Chem. Eur. J.* **2003**, *9*, 1893; f) D. Tasis, N. Tagmatarchis, V. Georgakilas, M. Prato, *Chem. Eur. J.* **2003**, *9*, 4000; g) *Carbon Nanotubes* (Eds.: S. Reich, C. Thomsen, J. Maultzsch), Wiley-VCH, Berlin, **2004**.
[3] N. Nakashima, *Int. J. Nanosci.* **2005**, *4*, 117.
[4] a) N. Nakashima, Y. Tomonari, H. Murakami, *Chem. Lett.* **2002**, 638; b) N. Nakashima, S. Okuzono, Y. Tomonari, H. Murakami, *Trans. Mater. Res. Soc. Jpn.* **2004**, *29*, 525; c) H. Murakami, T. Nomura, N. Nakashima, *Chem. Phys. Lett.* **2003**, *378*, 481; d) N. Nakashima, S. Okuzono, H. Murakami, T. Nakai, K. Yoshikawa, *Chem. Lett.* **2003**, *32*, 456; e) N. Nakashima, Y. Tanaka, Y. Tomonari, H. Murakami, H. Kataura, T. Sakaue, K. Yoshikawa, *J. Phys. Chem. B* **2005**, *109*, 13076.
[5] a) R. J. Chen, Y. Zhang, D. Wang, H. Dai, *J. Am. Chem. Soc.* **2001**, *123*, 3838; b) H. Xin, A. T. Woolley, *J. Am. Chem. Soc.* **2003**, *125*, 8710; c) F. J. Gómez, R. J. Chen, D. Wang, R. M. Waymouth, H. Dai, *Chem. Commun.* **2003**, 190; d) P. Petrov, F. Stassin, C. Pagnoulle, R. Jérôme, *Chem. Commun.* **2003**, 2904; e) L. Liu, T. Wang, J. Li, Z.-X. Guo, L. Dai, D. Zhang, D. Zhu, *Chem. Phys. Lett.* **2003**, *367*, 747; f) K. A. S. Fernando, Y. Lin, W. Wang, S. Kumar, B. Zhou, S.-Y. Xie, L. T. Cureton, Y.-P. Sun, *J. Am. Chem. Soc.* **2004**, *126*, 10234; g) M. Álvaro, P. Atienzar, J. L. Bourdelande, H. García, *Chem. Phys. Lett.* **2004**, *384*, 119; h) L. S. Fifield, L. R. Dalton, R. S. Addleman, R. A. Galhotra, M. H. Engelhard, G. E. Fryxell, C. L. Aardahl, *J. Phys. Chem. B* **2004**, *108*, 8737; i) A. B. Artyukhin, O. Bakajin, P. Stroeve, A. Noy, *Langmuir* **2004**, *20*, 1442.
[6] a) J. Zhang, J.-K. Lee, Y. Wu, R. W. Murray, *Nano Lett.* **2003**, *3*, 403; b) T. G. Hedderman, S. M. Keogh, G. Chambers, H. J. Byrne, *J. Phys. Chem. B* **2004**, *108*, 18860.
[7] a) D. M. Guldi, G. N. A. Rahman, J. Ramey, M. Marcaccio, D. Paolucci, F. Paolucci, S. Qin, W. T. Ford, D. Balbinot, N. Jux, N. Tagmatarchis, M. Prato, *Chem. Commun.* **2004**, 2004; b) D. M. Guldi, H. Taieb, G. M. A. Rahman, N. Tagmatarchis, M. Prato, *Adv. Mater.* **2005**, *17*, 871; c) D. Baskaran, J. W. Mays, X. P. Zhang, M. S. Bratcher, *J. Am. Chem. Soc.* **2005**, *127*, 6916; d) A. Satake, Y. Miyajima, Y. Kobuke, *Chem. Mater.* **2005**, *17*, 716.
[8] a) V. Krstic, G. S. Duesberg, J. Muster, M. Burghard, S. Roth, *Chem. Mater.* **1998**, *10*, 2338; b) N. Nakashima, H. Kobae, T. Sagara, H. Murakami, *ChemPhysChem* **2002**, *3*, 456; c) M. J. O'Connell, S. M. Bachio, C. B. Huffman, V. C. Moore, M. S. Strano, E. H. Haroz, K. L. Rialon, P. J. Boul, W. H. Noon, C. Kittrell, J. Ma, R. H. Hauge, R. B. Weisman, R. E. Smalley, *Science* **2002**, *297*, 593; d) S. M. Bachilo, M. S. Strano, C. Kittrell, R. H. Hauge, R. E. Smalley, R. B. Weisman, *Science* **2002**, *298*, 2361; e) M. F. Islam, E. Rojas, D. M. Bergey, A. T. Johnson, A. G. Yodh, *Nano Lett.* **2003**, *3*, 269; f) V. C. Moore, M. S. Strano, E. H. Haroz, R. H. Hauge, R. E. Smalley, *Nano Lett.* **2003**, *3*, 1379; g) R. B. Weisman, S. M. Bachilo, *Nano Lett.* **2003**, *3*, 1235; h) C. Richard, F. Balavoine, P. Schultz, T. W. Ebbesen, C. Mioskowski, *Science* **2003**, *300*, 775; i) K. Yurekli, C. A. Mitchell, R. Krishnamoorti, *J. Am. Chem. Soc.* **2004**, *126*, 9902; j) M. S. Strano, C. B. Huffman, V. C. Moore, M. J. O'Connell, E. H. Haroz, J. Hubbard, M. Miller, K. Rialon, C. Kittrell, S. Ramesh, R. H. Hauge, R. E. Smalley, *J. Phys. Chem. B* **2003**, *107*, 6979.
[9] a) D. M. Guldi, G. M. A. Rahman, N. Jux, N. Tagmatarchis, M. Prao, *Angew. Chem.* **2004**, *116*, 5642; *Angew. Chem. Int. Ed.* **2004**, *43*, 5526; b) D. M. Guldi, G. M. A. Rahman, N. Jux, D. Balbinot, N. Tagmatarchis, M. Prato, *Chem. Commun.* **2005**, 2038.
[10] a) D. M. Guldi, G. M. A. Rahman, M. Prato, N. Jux, S. Qin, W. Ford, *Angew. Chem.* **2005**, *117*, 2051; *Angew. Chem. Int. Ed.* **2005**, *44*, 2015; b) G. M. A. Rahman, D. M. Guldi, R. Cagnoli, A. Mucci, L. Schenetti, L. Vaccari, M. Prato, *J. Am. Chem. Soc.* **2005**, *127*, 10051.
[11] H. Li, B. Zhou, Y. Lin, L. Gu, W. Wang, K. A. S. Fernando, S. Kumar, L. F. Allard, Y.-P. Sun, *J. Am. Chem. Soc.* **2004**, *126*, 1014.
[12] H. Paloniemi, T. Ääriralo, T. Laiho, H. Like, N. Kocharova, K. Haapakka, F. Terzi, R. Seeber, J. Lukkari, *J. Phys. Chem. B* **2005**, *109*, 8634.
[13] I. W. Chiang, B. E. Brinson, A. Y. Huang, P. A. Willis, M. J. Bronikowski, J. L. Margrave, R. E. Smalley, R. H. Hauge, *J. Phys. Chem. B* **2001**, *105*, 8297.
[14] T. Ando, *J. Phys. Soc. Jpn.* **1997**, *66*, 1066.
[15] a) *Photophysics of Aromatic Molecules* (Ed.: J. B. Birks), John Wiley, New York, **1970**; b) *Principles of Fluorescence Spectroscopy* (Ed.: J. R. Lakowicz), Kluwer Academic/Plenum, **1999**.
[16] a) L. Qu, R. B. Martin, W. Huang, K. Fu, D. Zweifel, Y. Lin, Y.-P. Sun, C. E. Bunker, B. A. Harruff, J. R. Gord, L. F. Allard, *J. Chem. Phys.* **2002**, *117*, 8089; b) R. B. Martin, L. Qu, Y. Lin, B. A. Harruff, C. E. Bunker, J. R. Gord, L. F. Allard, Y.-P. Sun, *J. Phys. Chem. B* **2004**, *108*, 11447.
[17] H. Li, R. B. Martin, B. A. Harruff, R. A. Carino, L. F. Allrd, Y.-P. Sun, *Adv. Mater.* **2004**, *16*, 896.
[18] Y. Miyauchi, S. Chiashi, Y. Murakami, Y. Hayashida, S. Maruyama, *Chem. Phys. Lett.* **2004**, *387*, 198.
[19] a) J. C. Ma, D. A. Dougherty, *Chem. Rev.* **1997**, *97*, 1303; b) T. Fukushima, A. Kosaka, Y. Ishimura, T. Yamamoto, T. Takigawa, N. Ishii, T. Aida, *Science* **2003**, *300*, 2072.

Received: September 24, 2005
Published online: March 21, 2006

